

ID-Patch: Robust ID Association for Group Photo Personalization

Yimeng Zhang^{1,2,*}, Tiancheng Zhi¹, Jing Liu¹, Shen Sang¹,
Liming Jiang¹, Qing Yan¹, Sijia Liu², Linjie Luo¹

¹ ByteDance Inc., ² Michigan State University

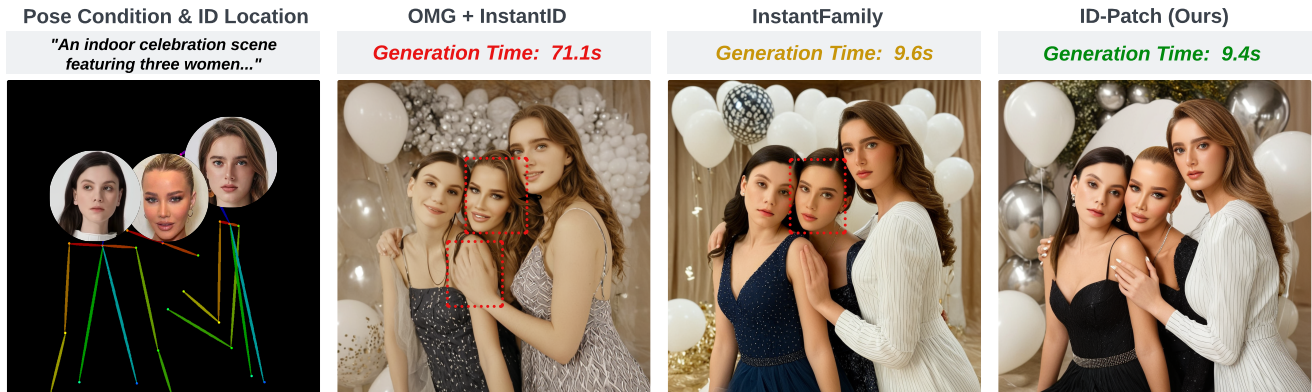


Figure 1. Comparison with state-of-the-art multi-identity generation methods. From left to right: the condition inputs followed by results generated using OMG [19] (with InstantID [41]), InstantFamily [17], and our proposed ID-Patch approach. Red dashed boxes highlight failures. OMG fails to preserve the hairstyles of the middle person, and creates artifacts for the right woman’s hand, possibly because of the inconsistency between its generation stages (explained in Fig. 2). InstantFamily suffers from ID leakage, resulting in the incorrect ID of the middle person. Our approach preserves the detailed identity of each person. In addition, our approach is 7 times faster than OMG and has less computational overhead than InstantFamily.

Abstract

The ability to synthesize personalized group photos and specify the positions of each identity offers immense creative potential. While such imagery can be visually appealing, it presents significant challenges for existing technologies. A persistent issue is identity (ID) leakage, where injected facial features interfere with one another, resulting in low face resemblance, incorrect positioning, and visual artifacts. Existing methods suffer from limitations such as the reliance on segmentation models, increased runtime, or a high probability of ID leakage. To address these challenges, we propose ID-Patch, a novel method that provides robust association between identities and 2D positions. Our approach generates an ID patch and ID embeddings from the same facial features: the ID patch is positioned on the conditional image for precise spatial control, while the ID embeddings integrate with text embeddings to ensure high resemblance. Experimental results demonstrate that ID-Patch surpasses baseline methods across met-

rics, such as face ID resemblance, ID-position association accuracy, and generation efficiency. Project Page is: <https://byteaigc.github.io/ID-Patch/>

1. Introduction

Personalized group photo generation has wide-ranging applications in entertainment, social media, and virtual reality. For example, users might want to create a group photo of friends at a virtual party, even if some could not attend in person. This enables the creation of engaging and memorable content that reflects real-life social interactions and relationships. However, this task poses significant challenges, particularly the risk of identity (ID) leakage, where the ID information of one individual inadvertently affects the representation of another at a different position. Such blending compromises the distinctiveness and accuracy of each person’s features. Besides, being able to specify the position of each identity in the image is an important function when users want to create a specific layout of people. Incorrect positioning of identities may lead to undesired results.

*Work done during internship at ByteDance.

State-of-the-art group photo personalization methods largely rely on diffusion models [3, 6, 16, 26, 37, 38], which deliver superior visual quality when paired with effective prompt engineering [4, 8, 25, 27, 34]. To address the issue of ID leakage, OMG [19] proposes a two-stage workflow: First, it generates an image without ID injection. Then, it estimates segmentation masks for the individuals in the image and subsequently injects the IDs into each segmented region. However, it depends on a segmentation model, which might fail in challenging cases. Besides, the content generated in the two stages may conflict with each other, leading to reduced visual fidelity. See Fig. 1 and Fig. 2 for example. Moreover, OMG requires running the denoising process separately for each identity, resulting in a runtime that increases linearly with the number of people. Alternatively, InstantFamily [17] employs a single-pass generation strategy by manipulating cross-attention masks. This approach uses approximate head region masks for each ID to direct pixel attention exclusively to specific ID embeddings derived from facial features. However, it struggles to prevent ID leakage due to two key issues: (1) imprecise masks or close proximity of faces, which can cause overlaps, and (2) unintended information propagation through self-attention and convolutional layers. Please see Fig. 1 and Fig. 3 for more details.

In response to these limitations, we propose a novel method named ID-Patch, designed for efficient and robust ID-position association in group photo generation. Our idea is to let the model learn to associate IDs with their spatially designated locations. Specifically, we project facial features onto a small RGB patch called ID patch and token embeddings called ID embeddings. The ID patches are placed onto the conditioning image of a ControlNet [49] according to face locations to ensure precise position control of IDs within the generated images. ID embeddings are integrated with text embeddings to enhance facial details. Our ID-Patch method seamlessly integrates with various types of spatial conditions, such as poses, canny edges or depth map, enhancing the robustness and flexibility of our method.

We summarize our key **contributions** as follows:

- Introduction of ID-Patch, an innovative method for multi-ID image generation that directly links face ID features with their corresponding locations using visual patches in conditioning images, ensuring better resemblance and accurate position control.
- Our proposed approach enhances the efficiency of multi-ID image generation, by merely adding ID patches to the ControlNet conditioning image and concatenating ID embeddings with text embeddings.
- Removal of the reliance on auxiliary segmentation models, requiring only a single point for ID position control, as opposed to segmented masks or head bounding boxes.
- Experimental results demonstrate the superiority of our

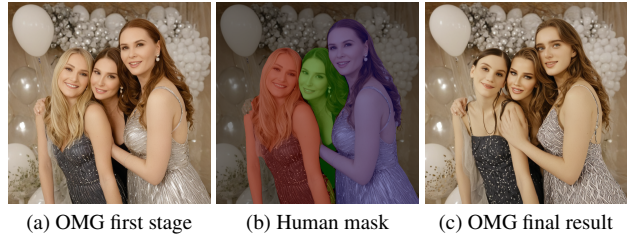


Figure 2. Why does OMG fail in Fig. 1? OMG relies on a first stage result (no ID awareness) and its human segmentation to control layout. The second stage paints injected IDs within corresponding masks. However, the second pass may conflict with the first stage semantics, leading to deteriorated ID resemblance (long hair in the middle of image (c)) or artifacts (hand in the middle).



Figure 3. ID leakage of InstantFamily [17]. The text prompt describes a man and a woman, and ID (a) is injected into the left man. However, in (b), InstantFamily suffers from ID leakage problem (right woman is incorrect) even though the cross attention mask (red box) has been manipulated to cover only the man’s face region. (c) Our method shows a properly generated result.

proposed ID-Patch over baseline methods in achieving higher fidelity in ID resemblance and higher robustness in position control, particularly in complex images featuring multiple identities.

2. Related Work

Single-ID Personalization. The personalization of diffusion models has emerged as a popular research topic. Fine-tuning or optimization based methods [9, 10, 32, 33, 44] have the potential to reach high quality results in terms of ID resemblance, but are time-consuming. Inference-only methods [15, 23, 28, 41, 43, 46, 47, 50] eliminate the fine-tuning process usually by encoding the concept into token embeddings and injecting them into the diffusion models via cross-attention. However, most of these works focus on single concept injection rather than group photo generation. **Multi-ID Personalization.** The main challenge of personalized group photo generation is ID blending, i.e., the identity information of person A may affect the generation of person B at another position. To resolve this issue, OMG [19] adopts a two-stage solution. First, a non-customized image is generated and masks of each person are extracted. Second, masked regions are painted using separate cus-

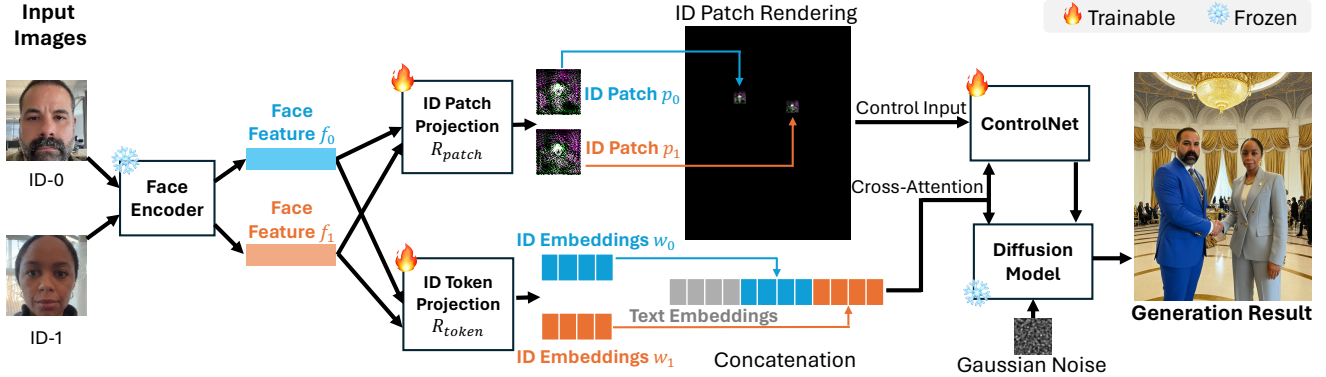


Figure 4. Our pipeline. Given a text prompt (e.g. two people shaking hands), N face images and locations, we generate an image with N IDs. We extract face features for each ID and project them into ID patches and ID embeddings. ID patches are rendered on a black canvas (or added on top of a pose image) according to face locations and sent into a ControlNet to control the positions of generated faces. ID embeddings are appended to text embeddings to provide detailed face information to the diffusion model and ControlNet via cross-attention.

tomized models and stitched together. This approach is slow and conflicts between stages may cause identity loss. Additionally, it relies on a segmentation module, which may fail in challenging cases. To avoid running separate customized models, recent works [14, 40, 45] let the network to learn to attend to specific concept tokens by supervising the attention mask using segmentation or ID routing. However, these methods do not allow the specification of the accurate locations of each ID. Although they can be combined with pose conditions, describing the assignment of IDs to positions in text may be hard. InstantFamily [17] provides an opportunity to specify the approximate location of each ID by manipulating the attention masks during both training and inference. However, no constraints have been imposed to avoid the ID leakage through self-attention and convolutional layers, leading to ID blending, omitting or swapping. **Multiple General Concepts.** Besides human generation, there are series of work focusing on the customization of multiple general concepts [1, 2, 7, 12, 13, 20, 24, 39, 45] and grounded image generation [2, 22, 42] associating objects with positions. GLIGEN [22] integrates grounding tokens, which align textual prompts with specific image regions. SpaText [2] and InstanceDiffusion [42] allows users to define the placement and attributes of objects. However, these concepts are usually semantically distinct while it is hard to describe the human identities in text and subtle details matter.

3. Method

In this section, we first outline some preliminaries about text-to-image diffusion models and ControlNets. Subsequently, we detail the problem formulation for multi-ID image generation and the design of our modules, including the ID patch and ID embeddings, as well as the training and inference schemes.

3.1. Preliminaries

Latent diffusion models (LDMs). LDMs [31] are image generation models that can incorporate conditioning signals into the generation process. Specifically, during training, an encoder \mathcal{E} of variational autoencoder (VAE) [18] encodes an image into a latent space, and a neural network $\epsilon_\theta(z_t, t, c)$ performs the denoising process within this latent space. It attempts to predict the original Gaussian noise ϵ from a noisy latent variable z_t , where t represents the diffusion timestep, and c is the conditioning signal, injected via cross-attention. The loss function for an LDM is defined as:

$$L_{\text{LDM}} = \mathbb{E}_{\mathcal{E}, \epsilon \sim \mathcal{N}(0,1), t} [\|\epsilon - \epsilon_\theta(z_t, t, c)\|_2^2] \quad (1)$$

ControlNet. The incorporation of ControlNet [49] into diffusion models marks a significant advancement in controlled image synthesis. ControlNet is designed to steer the image generation process by applying spatial conditioning signals such as rasterized pose images, depth maps, or canny edges. It introduces a control network that processes these signals and adds their features to the base model’s intermediate results. The control network is a trainable copy of the base model’s encoder layers and is initialized with zero convolution. This effective integration achieves high quality controlled generation.

3.2. Multi-ID Image Generation

This paper focuses on efficiently and effectively addressing the problem of multi-ID image generation utilizing conditioning signals that include text prompts, identity features, and face locations. The inputs to our model comprise text prompt embeddings c_t , facial features $c_f = (f_0, f_1, \dots, f_{N-1})$ for N distinct identities, and their corresponding facial locations $c_l = (l_0, l_1, \dots, l_{N-1})$. The facial location $l_i = (x_i, y_i)$ identifies the xy-coordinates of the nose tip for each identity within the intended image. The



Figure 5. Effectiveness of ID embedding. Without ID embeddings, one can distinguish between the two people but the resemblance is low. Incorporating ID embeddings significantly improves face resemblance.

goal is to synthesize an image following the text description with each given face located in the designated place.

3.2.1 ID Patches and ID Embeddings

As discussed in Sec. 3.1, ControlNet effectively integrates spatial conditional signals into diffusion models. Building on this capability, we introduce a method to encode ID location information using condition images, subsequently processed by ControlNet to guide ID localization within the generated image. Our approach features ID conditions manifesting as both patches and embeddings. Specifically, ID patches, precisely aligned with facial locations, are integrated via ControlNet to ensure accurate identity localization, while ID embeddings are utilized via cross-attention mechanisms in the LDM to enhance the detailed representation of facial features, as illustrated in Fig. 4.

Both ID patches and ID embeddings are derived from facial features, enabling a synergistic association between them, with both projection processes facilitated by the Perceiver Resampler [46]. For ID patches, we convert the facial feature f_i into an identity-specific patch $p_i \in \mathbb{R}^{P \times P \times 3}$, functioning similarly to a QR code, uniquely identifying each person and easily distinguishable from others. These ID patches are placed on a black canvas at specified facial locations to create an image I , which then serves as the conditioning input for ControlNet, thereby providing precise identity localization information.

As depicted in Fig. 5, while ID patches alone are generally sufficient for distinguishing between identities, they may not always achieve optimal results in generating images with high ID resemblance. To address this limitation, and inspired by InstantFamily [17], we also incorporate ID embeddings. These embeddings are designed to inject detailed facial appearance information into the diffusion model, thus enhancing the resemblance of the generated identities to their real-life counterparts. Specifi-

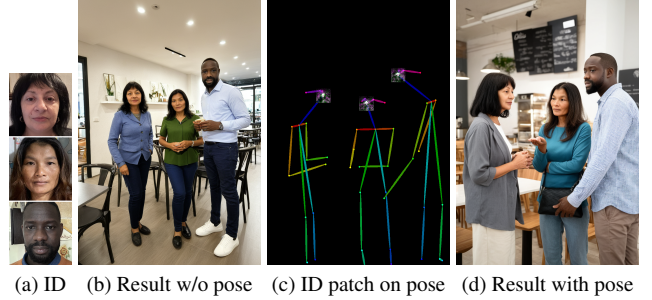


Figure 6. ID-Patch combined with pose conditions. Provided with user ID images in (a), our method can generate results with only the specifications of nose tip locations as shown in (b). Merging ID patches with pose images (c) enhances spatial control over the generated results as seen in (d), without incurring any computational overhead.

cally, ID embeddings $w_i \in \mathbb{R}^{2048 \times M}$, share the same token dimension 2048 as the SDXL text embeddings. As shown in Fig. 4, these embeddings are appended to text embeddings c_t to form an extended text embedding $c'_t = [c_t, w_0, w_1, \dots, w_{N-1}]$, which is then fed into both the UNet and ControlNet through cross-attention mechanisms.

Since human pose conditions are often utilized to enhance group photo generation, we can combine our ID-Patch approach with the pose conditions for multi-id image generation. As illustrated in Fig. 6, the ID patches can be overlaid onto a pose-conditioned image, creating a composite condition image that encodes both identity positioning and pose information. It is important to mention that while our method can incorporate pose information, it does not inherently require it; pose is just an optional enhancement, one can also choose other conditions like canny edge, depth map for specific applications. The adaptability of our ID-Patch approach presents enhanced control over generated results yet without incurring the extra overhead of an additional ControlNet branch.

3.2.2 Two-Stage Training and Inference

The training of our model employs a conventional diffusion loss function, defined as follows:

$$L = \mathbb{E}_{\mathcal{E}, \epsilon \sim \mathcal{N}(0,1), t} [\|\epsilon - \epsilon\theta(z_t, t, I, c'_t)\|_2^2] \quad (2)$$

Initially, one might consider training the models end-to-end from scratch. However, our experiments reveal that such a method does not consistently ensure accurate ID localization, as depicted in Fig. 7. This shortcoming likely stems from the network’s tendency to preferentially inject ID information into ID embeddings, rather than ID patches, resulting in non-distinctive ID patches that could potentially confuse ControlNet. In the single-stage model, as shown in Fig. 7, the ID patches exhibit only subtle differences between different individuals.



Figure 7. Two-stage training to improve positioning robustness. Given pose and ID conditions in (a), single-stage training cannot fully prevent the incorrect face positioning issue. For example, in (b), the man is mistakenly placed at the central bottom position, generating an inharmonious result. (c) Two-stage training is introduced to solve this problem. As can be seen on the top row of this figure, the ID patches from our two-stage training approach are visually more distinguishable from each other, compared to the ones from single-stage training. Our experimental results prove that this is critical in solving the ID leak issues.

To resolve this, we introduce a two-stage training approach. In the initial stage, ID embeddings are omitted, compelling the network to prioritize the incorporation of ID information into ID patches, thereby enhancing their distinctiveness. In the subsequent stage, ID embeddings are introduced and the model is fine-tuned to further improve the resemblance of the generated images.

We also implement a two-stage inference process that further enhances performance. Specifically, during the first $\sim 20\%$ of the timesteps, only ID patches are utilized. This focuses the early denoising steps on establishing basic ID localization without the detailed facial features encoded in ID embeddings, which are not as effective in the initial phases. For the remaining timesteps, both ID patches and ID embeddings are employed, allowing the finer facial details to be incorporated as the image clarity improves. This strategy not only ensures better ID localization but also minimizes interference with text conditions, thus enhancing the model’s ability to follow text prompts.

4. Experiments

4.1. Settings

Implementation details. Facial features f_i we use are 512-dimensional vectors derived from ArcFace [5]. During training, we utilize the SDXL diffusion model [29]. During the inference phase, we employ the further finetuned SDXL, namely Juggernaut-X-v10¹, as base model to enhance portrait quality. The inference process involves 50 timesteps.

¹ <https://huggingface.co/RunDiffusion/Juggernaut-X-v10>

Table 1. Performance comparison across four dimensions: identity resemblance, ID-position association accuracy, text alignment, and generation time. For qualitative metrics to evaluate similarity or accuracy, higher is better. Our approach significantly outperforms baseline methods in terms of resemblance, association, and generation time, with similar text alignment scores.

| Methods | ID \uparrow | Association \uparrow | Text \uparrow | Time (s) \downarrow |
|-----------------|---------------|------------------------|-----------------|-----------------------|
| OMG + InstantID | 0.644 | 0.926 | 0.271 | 84.83 |
| InstantFamily | 0.683 | 0.862 | 0.278 | 10.02 |
| ID-Patch (Ours) | 0.751 | 0.958 | 0.273 | 9.69 |

As mentioned in Sec. 3.2.2, we divide these timesteps into two phases to regulate the influence of identity features: the initial 20% of timesteps operate without ID token embeddings to focus on the general style, followed by the remaining timesteps which incorporate ID token embeddings to refine the identity-specific aspects of the images. The default size of ID-patch is $P \times P = 64 \times 64$ and the default length of ID embeddings is $M = 16$.

Dataset. Our training set consists of 17 million single-person and 1.95 million multi-person images. These images are obtained from purchased data and publicly available sources. For evaluation, we utilize two specialized datasets: 1) *Style Dataset* comprises 40 styles with pose and text prompt definitions, ranging from one to eight faces. 2) *Identity Dataset* includes 600 unique identities representing a variety of races and genders. Each style is paired with 20 randomly sampled unique identity combinations for quantitative evaluation.

Baselines. Our analysis includes two state-of-the-art multi-ID generation methods as baselines: 1) **OMG** [19]: This method incorporates multiple identity features into separate segmented regions through latent stitching. It can be paired with a single ID injection method InstantID [41] for multi-ID generation. 2) **InstantFamily** [17]: This approach employs coarse attention masks within cross-attention layers, a mandatory process that ensures distinct identity features are injected into different image instances effectively.

Evaluation Metrics. We evaluate the methods in a pose-conditioned setting, because pose is a requirement of InstantFamily, and without pose condition, OMG is not able to generate faces at specified locations for its first stage. Besides, pose condition makes the head size consistent, which is easier for resemblance evaluation and reduces the impact of head sizes on generation quality. For comprehensive evaluation, we consider four critical dimensions: 1) Identity resemblance: we measure the identity resemblance by calculating the cosine similarity (CosSim) between the facial features of faces in the generated images and the reference faces. For fairness, we use FaceNet [35], a face model different from the ArcFace model used for training. 2) Association accuracy: we assess the accuracy of identity-position association in generated images by ensuring that

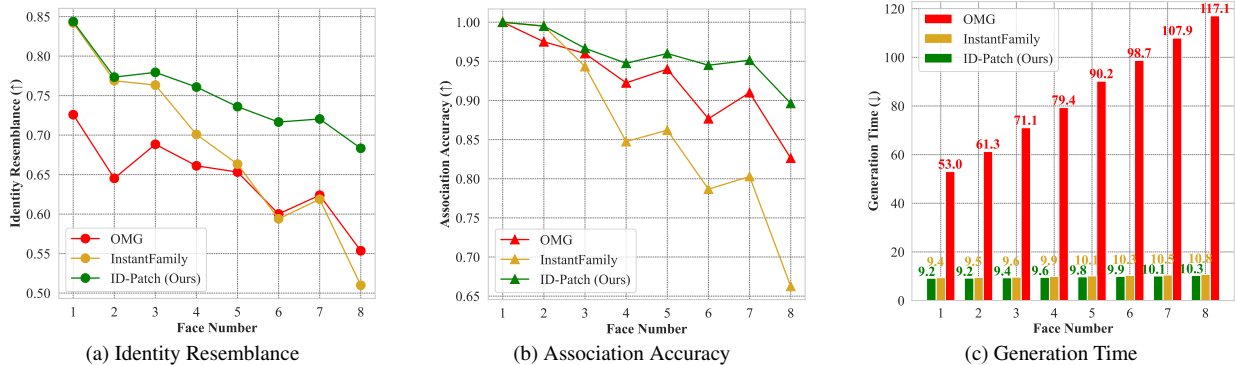


Figure 8. Performance evaluation of different model generations from three different aspects: identity resemblance, location accuracy, and generation time. As face number increases, the ID and location metric scores of OMG and Instantfamily drop much more significantly than our approach. Our approach also achieves near-constant generation time, in contrast to OMG’s linearly increasing running time.

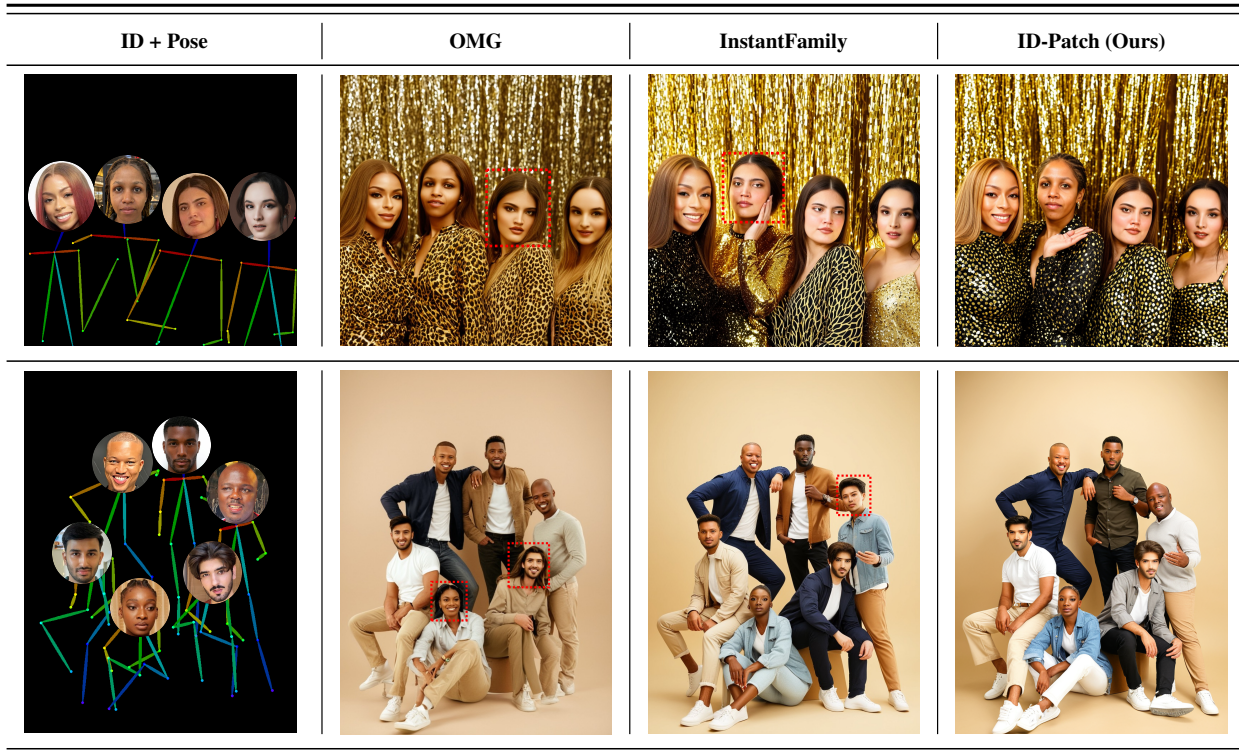


Figure 9. Comparison with baselines on pose-conditioned generation, where red dashed boxes highlight instances with low identity resemblance. In row 1, OMG fails to preserve the face shape of the third woman (from left to right) because its first stage result conflicts with this ID’s face shape. InstantFamily incorrectly generates the second person because of the ID leakage from the third woman. In row 2, OMG does not generate correct hair styles and accurate facial features for the two people in the red boxes, while InstantFamily generates the wrong ID in the red box.

the generated faces are most similar to their assigned counterparts, compared to all other input faces used in the generation process. In other words, we calculate the similarity between the i -th generated face and the j -th input face. Let $s(i) = \arg \max_{0 \leq j \leq N-1} \text{CosSim}(\tilde{f}_i^{\text{gen}}, \tilde{f}_j)$ be the face index among all input faces that is most similar to the i -th generated face, where $\tilde{f}_i^{\text{gen}}, \tilde{f}_j$ denote the FaceNet features of the i -th generated face and the j -th input face respec-

tively, and N is the number of faces in this image. When $s(i) = i$, the i -th generated face has the correct association. The identity-position association accuracy is defined as:

$$\frac{1}{N} \sum_{i=0}^{N-1} \mathbf{1}\{i = s(i)\} \quad (3)$$

This measurement assesses the correct placement of each identity within the image. 3) Text alignment: this met-

Table 2. Ablation study results for our proposed ID-Patch variants, designed to assess the impact of different modules (patch projection and token projection) and training/inferencing schemes on the performance of multi-ID image generation. The full method achieves the best ID resemblance and ID-position association, indicating the necessity of each module.

| Variants | ID \uparrow | Association \uparrow | Text \uparrow |
|------------------------|---------------|------------------------|-----------------|
| No patch projection | 0.368 | 0.345 | 0.271 |
| No token projection | 0.565 | 0.895 | 0.284 |
| Single stage training | 0.660 | 0.784 | 0.271 |
| Single stage inference | 0.750 | 0.957 | 0.270 |
| FULL | 0.751 | 0.958 | 0.273 |

ric evaluates the alignment between the textual context of the image generation prompt and the visual output. Cosine similarity is used to compare textual features extracted by the CLIP text encoder with visual features extracted by the CLIP image encoder from the generated images [30]. 4) Generation time: we measure the efficiency by recording the time (in seconds) required to generate an image on an NVIDIA A100 GPU, excluding the time taken for model loading and image I/O.

4.2. Comparison with Baselines

As listed in **Tab. 1**, ID-Patch excels in identity and association metrics with scores of 0.751 and 0.958, respectively, showcasing its robust capability to maintain identity consistency and achieve precise placement in generated images. There is no significant difference in text alignment scores between compared methods. Notably, ID-Patch achieves the fastest image generation time.

Further details on the performance with varying face numbers are shown in **Fig. 8**. As we observed no deterioration in text alignment with an increase in the number of faces across all methods, we have relegated the corresponding figure to the appendix. As the number of faces increases, both OMG and InstantFamily experience significant performance drops due to ID leakage. Although ID-Patch also shows a decline, it is less severe, mainly because the increase in face numbers reduces the average face area, adversely affecting the quality of smaller faces produced by the SDXL models. Moreover, the presence of more faces slightly extends the image generation time due to the increased demand for facial feature extraction. InstantFamily is slightly slower than our approach due to the overhead of masked attention. For OMG, injecting identity features into designated segmented areas causes a substantial increase in generation time; it takes about 2 minutes to generate an image with eight people, whereas ID-Patch requires only about 10 seconds. See **Fig. 9** for visual comparisons.

4.3. Ablation Study

We conduct an ablation study on variants of the proposed method in **Tab. 2**. The performance notably degrades when patch projection is omitted, leading to poor location alignment as the algorithm attempts to infer ID locations based on indirect cues such as gender and pose. Similarly, omitting token projection reduces resemblance by eliminating essential facial details, quantitatively validates the finding of **Fig. 5**. Single-stage training results in indistinguishable ID patches (as shown in **Fig. 7**), which impairs effective positioning. Our proposed ID-Patch, which utilizes two-stage inference, significantly enhances both text alignment and ID positioning over its single-stage counterpart, although it does not alter ID resemblance. This may be because ID embeddings contribute minimally to facial detail representation in the initial denoising steps but are more influential in subsequent text following and ID positioning.

4.4. Pose-Free Generation

Our ID-Patch model can be operated effectively without the need for pose conditioning, a flexibility that permits its integration with other conditions for image generation. This capability enables the use of ID-Patch in versatile configurations, whether plug-and-play or co-trained, which we will explore in subsequent subsections.

In the pose-free mode, the ControlNet uses a conditioning image that solely features ID patches against a black background. The placement of each ID patch at the tip of the nose ensures accurate preservation of facial locations during image synthesis, while head sizes and poses are variably generated based on the initial noise. As illustrated in **Fig. 10**, this methodology allows our model to produce aesthetically pleasing group photographs of different number of individuals across a variety of settings, demonstrating the robustness and adaptability of our approach.

The pose-free version of ID-Patch is designed to be compatible with other ControlNets (**plug-and-play**). As illustrated in **Fig. 11**, it is possible to combine our ID-Patch ControlNet the Canny edge ControlNet to achieve more precise control over the final image outcomes.

4.5. Limitations

As illustrated in **Fig. 12**, our method encounters two primary limitations. First, our implementation is based on the SDXL model, which occasionally produces inaccuracies in body and finger anatomy. Transitioning to a more advanced base model could potentially rectify this issue. Second, facial features in the current model may incorporate lighting and expression details that are not fully separated from identity information, potentially compromising the generation quality. Enriching our training dataset with multiple images of the same identities, showcasing varied expressions and lighting conditions, might help alleviate this problem.

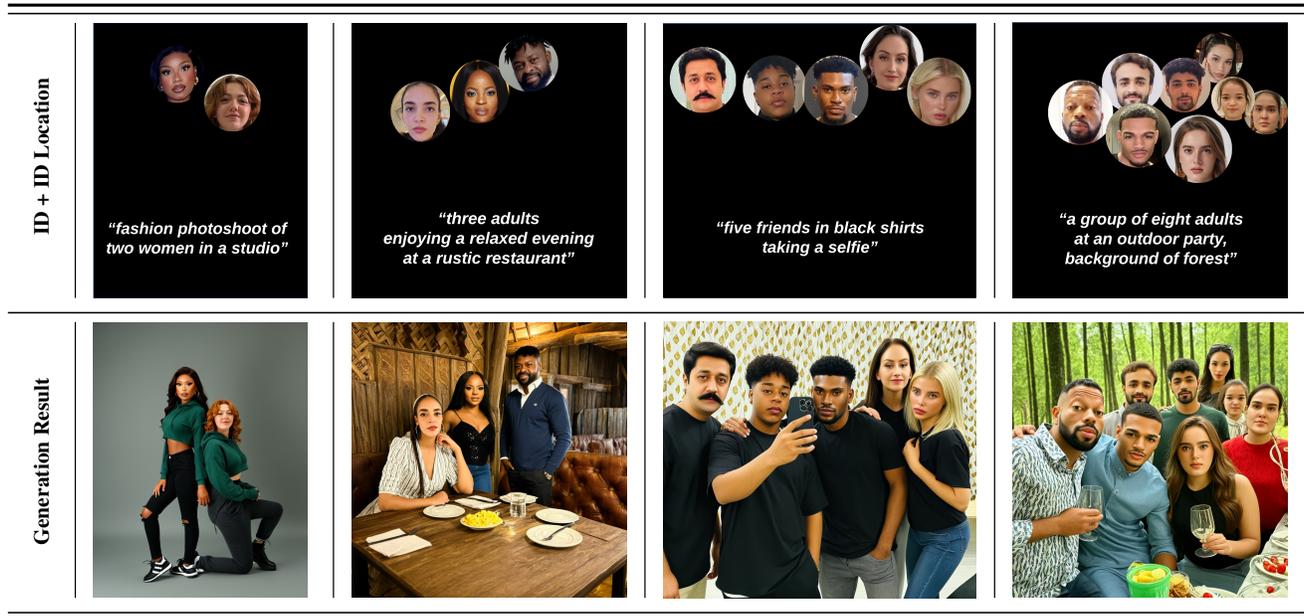


Figure 10. ID-Patch pose-free generation. Here the condition image is only ID patches rendered onto a black canvas without any pose condition. The generation is conditioned on individual face locations while corresponding head sizes and body poses are inferred implicitly. Our method can accommodate a large number of people with diverse ethnic backgrounds, yet generating visually appealing group photo results. See “Evaluation Metrics” for reasons why we compare with baseline approaches only in pose-conditioned settings.



Figure 11. Combination of pose-free ID-Patch ControlNet and pretrained Canny edge ControlNet. We can generate background and clothing details, with high quality ID injection.

Although the resemblance has been improved with our approach, there still exists a performance gap between generating a single person and multiple people (Fig. 8 (a)). This means generating personalized group photo remains a challenging problem and requires further study.

5. Conclusion

In conclusion, our novel method, ID-Patch, markedly enhances identity resemblance and positioning in group photo generation. By embedding each identity feature within a distinct patch and utilizing ControlNet to accurately place each identity at the designated spatial locations, we successfully reduce ID leakage. Our approach seamlessly in-



Figure 12. Limitations. (a) Abnormal anatomy can be found in complex scenes, e.g. the forearms in the red box. (b) When input faces contain strong shadows, our method struggles to fully disentangle user’s ID in generated result.

tegrates with additional conditioning signals such as pose control. Experimental results underscore the superiority of ID-Patch, particularly in complex scenarios involving more than three identities. This work paves the way for future explorations in multi-ID image generation. Potential future research directions include leveraging multiple images of the same individual from different angles to further enhance identity resemblance and simultaneously controlling location and facial expressions using the patch technique.

Societal Impact: Our work studies ID injection from a technical perspective and is not intended for malicious use. However, inappropriate usage might generate undesired fake images. Users should be aware of the ethical implications and use it responsibly.

References

- [1] Omri Avrahami, Kfir Aberman, Ohad Fried, Daniel Cohen-Or, and Dani Lischinski. Break-a-scene: Extracting multiple concepts from a single image. In *SIGGRAPH Asia 2023 Conference Papers*, pages 1–12, 2023. 3
- [2] Omri Avrahami, Thomas Hayes, Oran Gafni, Sonal Gupta, Yaniv Taigman, Devi Parikh, Dani Lischinski, Ohad Fried, and Xi Yin. Spatext: Spatio-textual representation for controllable image generation. In *Proceedings of the IEEE/CVF Conference on Computer Vision and Pattern Recognition*, pages 18370–18380, 2023. 3
- [3] Yogesh Balaji, Seungjun Nah, Xun Huang, Arash Vahdat, Jiaming Song, Qingsheng Zhang, Karsten Kreis, Miika Aittala, Timo Aila, Samuli Laine, et al. ediff-i: Text-to-image diffusion models with an ensemble of expert denoisers. *arXiv preprint arXiv:2211.01324*, 2022. 2
- [4] Junsong Chen, Jincheng Yu, Chongjian Ge, Lewei Yao, Enze Xie, Yue Wu, Zhongdao Wang, James Kwok, Ping Luo, Huchuan Lu, et al. Pixart- α : Fast training of diffusion transformer for photorealistic text-to-image synthesis. *arXiv preprint arXiv:2310.00426*, 2023. 2
- [5] Jiankang Deng, Jia Guo, Niannan Xue, and Stefanos Zafeiriou. Arcface: Additive angular margin loss for deep face recognition. In *Proceedings of the IEEE/CVF conference on computer vision and pattern recognition*, pages 4690–4699, 2019. 5
- [6] Prafulla Dhariwal and Alexander Nichol. Diffusion models beat gans on image synthesis. *Advances in neural information processing systems*, 34:8780–8794, 2021. 2
- [7] Gangui Ding, Canyu Zhao, Wen Wang, Zhen Yang, Zide Liu, Hao Chen, and Chunhua Shen. Freecustom: Tuning-free customized image generation for multi-concept composition. In *Proceedings of the IEEE/CVF Conference on Computer Vision and Pattern Recognition*, pages 9089–9098, 2024. 3
- [8] Patrick Esser, Sumith Kulal, Andreas Blattmann, Rahim Entezari, Jonas Müller, Harry Saini, Yam Levi, Dominik Lorenz, Axel Sauer, Frederic Boesel, et al. Scaling rectified flow transformers for high-resolution image synthesis, march 2024. URL <http://arxiv.org/abs/2403.03206>. 2
- [9] Rinon Gal, Yuval Alaluf, Yuval Atzmon, Or Patashnik, Amit H Bermano, Gal Chechik, and Daniel Cohen-Or. An image is worth one word: Personalizing text-to-image generation using textual inversion. *arXiv preprint arXiv:2208.01618*, 2022. 2
- [10] Rinon Gal, Moab Arar, Yuval Atzmon, Amit H Bermano, Gal Chechik, and Daniel Cohen-Or. Encoder-based domain tuning for fast personalization of text-to-image models. *ACM Transactions on Graphics (TOG)*, 42(4):1–13, 2023. 2
- [11] Zigang Geng, Ke Sun, Bin Xiao, Zhaoxiang Zhang, and Jingdong Wang. Bottom-up human pose estimation via disentangled keypoint regression. In *Proceedings of the IEEE/CVF conference on computer vision and pattern recognition*, pages 14676–14686, 2021. 12
- [12] Yuchao Gu, Xintao Wang, Jay Zhangjie Wu, Yujun Shi, Yunpeng Chen, Zihan Fan, Wuyou Xiao, Rui Zhao, Shuning Chang, Weijia Wu, et al. Mix-of-show: Decentralized low-rank adaptation for multi-concept customization of diffusion models. *Advances in Neural Information Processing Systems*, 36, 2024. 3
- [13] Ligong Han, Yinxiao Li, Han Zhang, Peyman Milanfar, Dimitris Metaxas, and Feng Yang. Svdiff: Compact parameter space for diffusion fine-tuning. In *Proceedings of the IEEE/CVF International Conference on Computer Vision*, pages 7323–7334, 2023. 3
- [14] Junjie He, Yifeng Geng, and Liefeng Bo. Unipor-trait: A unified framework for identity-preserving single- and multi-human image personalization. *arXiv preprint arXiv:2408.05939*, 2024. 3
- [15] Zecheng He, Bo Sun, Felix Juefei-Xu, Haoyu Ma, Ankit Ramchandani, Vincent Cheung, Siddharth Shah, Anmol Kalia, Harihar Subramanyam, Alireza Zareian, et al. Imagine yourself: Tuning-free personalized image generation. *arXiv preprint arXiv:2409.13346*, 2024. 2
- [16] Jonathan Ho, Ajay Jain, and Pieter Abbeel. Denoising diffusion probabilistic models. *Advances in neural information processing systems*, 33:6840–6851, 2020. 2
- [17] Chanran Kim, Jeongin Lee, Shichang Joung, Bongmo Kim, and Yeul-Min Baek. Instantfamily: Masked attention for zero-shot multi-id image generation. *arXiv preprint arXiv:2404.19427*, 2024. 1, 2, 3, 4, 5, 12
- [18] Diederik P Kingma. Auto-encoding variational bayes. *arXiv preprint arXiv:1312.6114*, 2013. 3
- [19] Zhe Kong, Yong Zhang, Tianyu Yang, Tao Wang, Kaihao Zhang, Bizhu Wu, Guanying Chen, Wei Liu, and Wenhan Luo. Omg: Occlusion-friendly personalized multi-concept generation in diffusion models. In *ECCV*, 2024. 1, 2, 5
- [20] Nupur Kumari, Bingliang Zhang, Richard Zhang, Eli Shechtman, and Jun-Yan Zhu. Multi-concept customization of text-to-image diffusion. In *Proceedings of the IEEE/CVF Conference on Computer Vision and Pattern Recognition*, pages 1931–1941, 2023. 3
- [21] Junnan Li, Dongxu Li, Silvio Savarese, and Steven Hoi. Bliip-2: Bootstrapping language-image pre-training with frozen image encoders and large language models. In *International conference on machine learning*, pages 19730–19742. PMLR, 2023. 12
- [22] Yuheng Li, Haotian Liu, Qingyang Wu, Fangzhou Mu, Jianwei Yang, Jianfeng Gao, Chunyuan Li, and Yong Jae Lee. Gligen: Open-set grounded text-to-image generation. In *Proceedings of the IEEE/CVF Conference on Computer Vision and Pattern Recognition*, pages 22511–22521, 2023. 3
- [23] Zhen Li, Mingdeng Cao, Xintao Wang, Zhongang Qi, Ming-Ming Cheng, and Ying Shan. Photomaker: Customizing realistic human photos via stacked id embedding. In *Proceedings of the IEEE/CVF Conference on Computer Vision and Pattern Recognition*, pages 8640–8650, 2024. 2
- [24] Zhiheng Liu, Ruili Feng, Kai Zhu, Yifei Zhang, Kecheng Zheng, Yu Liu, Deli Zhao, Jingren Zhou, and Yang Cao. Cones: Concept neurons in diffusion models for customized generation. *arXiv preprint arXiv:2303.05125*, 2023. 3
- [25] Nanye Ma, Mark Goldstein, Michael S Albergo, Nicholas M Boffi, Eric Vanden-Eijnden, and Saining Xie. Sit: Exploring flow and diffusion-based generative models with scalable

- interpolant transformers. *arXiv preprint arXiv:2401.08740*, 2024. 2
- [26] Alex Nichol, Prafulla Dhariwal, Aditya Ramesh, Pranav Shyam, Pamela Mishkin, Bob McGrew, Ilya Sutskever, and Mark Chen. Glide: Towards photorealistic image generation and editing with text-guided diffusion models. *arXiv preprint arXiv:2112.10741*, 2021. 2
- [27] William Peebles and Saining Xie. Scalable diffusion models with transformers. In *Proceedings of the IEEE/CVF International Conference on Computer Vision*, pages 4195–4205, 2023. 2
- [28] Xu Peng, Junwei Zhu, Boyuan Jiang, Ying Tai, Donghao Luo, Jiangning Zhang, Wei Lin, Taisong Jin, Chengjie Wang, and Rongrong Ji. Portraitbooth: A versatile portrait model for fast identity-preserved personalization. In *Proceedings of the IEEE/CVF Conference on Computer Vision and Pattern Recognition*, pages 27080–27090, 2024. 2
- [29] Dustin Podell, Zion English, Kyle Lacey, Andreas Blattmann, Tim Dockhorn, Jonas Müller, Joe Penna, and Robin Rombach. Sdxl: Improving latent diffusion models for high-resolution image synthesis. In *The Twelfth International Conference on Learning Representations*, 2024. 5, 12
- [30] Alec Radford, Jong Wook Kim, Chris Hallacy, Aditya Ramesh, Gabriel Goh, Sandhini Agarwal, Girish Sastry, Amanda Askell, Pamela Mishkin, Jack Clark, et al. Learning transferable visual models from natural language supervision. In *International conference on machine learning*, pages 8748–8763. PMLR, 2021. 7
- [31] Robin Rombach, Andreas Blattmann, Dominik Lorenz, Patrick Esser, and Björn Ommer. High-resolution image synthesis with latent diffusion models. In *Proceedings of the IEEE/CVF conference on computer vision and pattern recognition*, pages 10684–10695, 2022. 3
- [32] Nataniel Ruiz, Yuanzhen Li, Varun Jampani, Yael Pritch, Michael Rubinstein, and Kfir Aberman. Dreambooth: Fine tuning text-to-image diffusion models for subject-driven generation. In *Proceedings of the IEEE/CVF Conference on Computer Vision and Pattern Recognition*, pages 22500–22510, 2023. 2
- [33] Nataniel Ruiz, Yuanzhen Li, Varun Jampani, Wei Wei, Tingbo Hou, Yael Pritch, Neal Wadhwa, Michael Rubinstein, and Kfir Aberman. Hyperdreambooth: Hypernetworks for fast personalization of text-to-image models. In *Proceedings of the IEEE/CVF Conference on Computer Vision and Pattern Recognition*, pages 6527–6536, 2024. 2
- [34] Chitwan Saharia, William Chan, Saurabh Saxena, Lala Li, Jay Whang, Emily L Denton, Kamyar Ghasemipour, Raphael Gontijo Lopes, Burcu Karagol Ayan, Tim Salimans, et al. Photorealistic text-to-image diffusion models with deep language understanding. *Advances in Neural Information Processing Systems*, 35:36479–36494, 2022. 2
- [35] Florian Schroff, Dmitry Kalenichenko, and James Philbin. Facenet: A unified embedding for face recognition and clustering. In *Proceedings of the IEEE conference on computer vision and pattern recognition*, pages 815–823, 2015. 5
- [36] Noam Shazeer and Mitchell Stern. Adafactor: Adaptive learning rates with sublinear memory cost. In *International Conference on Machine Learning*, pages 4596–4604. PMLR, 2018. 12
- [37] Jascha Sohl-Dickstein, Eric Weiss, Niru Maheswaranathan, and Surya Ganguli. Deep unsupervised learning using nonequilibrium thermodynamics. In *International conference on machine learning*, pages 2256–2265. PMLR, 2015. 2
- [38] Jiaming Song, Chenlin Meng, and Stefano Ermon. Denoising diffusion implicit models. *arXiv preprint arXiv:2010.02502*, 2020. 2
- [39] Yoad Tewel, Rinon Gal, Gal Chechik, and Yuval Atzmon. Key-locked rank one editing for text-to-image personalization. In *ACM SIGGRAPH 2023 Conference Proceedings*, pages 1–11, 2023. 3
- [40] Kuan-Chieh Wang, Daniil Ostashev, Yuwei Fang, Sergey Tulyakov, and Kfir Aberman. Moa: Mixture-of-attention for subject-context disentanglement in personalized image generation. *arXiv preprint arXiv:2404.11565*, 2024. 3
- [41] Qixun Wang, Xu Bai, Haofan Wang, Zekui Qin, and Anthony Chen. Instantid: Zero-shot identity-preserving generation in seconds. *arXiv preprint arXiv:2401.07519*, 2024. 1, 2, 5
- [42] Xudong Wang, Trevor Darrell, Sai Saketh Rambhatla, Rohit Girdhar, and Ishan Misra. Instancediffusion: Instance-level control for image generation. In *Proceedings of the IEEE/CVF Conference on Computer Vision and Pattern Recognition (CVPR)*, pages 6232–6242, 2024. 3
- [43] Yuxiang Wei, Yabo Zhang, Zhilong Ji, Jinfeng Bai, Lei Zhang, and Wangmeng Zuo. Elite: Encoding visual concepts into textual embeddings for customized text-to-image generation. In *Proceedings of the IEEE/CVF International Conference on Computer Vision*, pages 15943–15953, 2023. 2
- [44] Yuxin Wen, Neel Jain, John Kirchenbauer, Micah Goldblum, Jonas Geiping, and Tom Goldstein. Hard prompts made easy: Gradient-based discrete optimization for prompt tuning and discovery. *Advances in Neural Information Processing Systems*, 36, 2024. 2
- [45] Guangxuan Xiao, Tianwei Yin, William T Freeman, Frédo Durand, and Song Han. Fastcomposer: Tuning-free multi-subject image generation with localized attention. *International Journal of Computer Vision*, pages 1–20, 2024. 3
- [46] Hu Ye, Jun Zhang, Sibio Liu, Xiao Han, and Wei Yang. Ip-adapter: Text compatible image prompt adapter for text-to-image diffusion models. *arXiv preprint arXiv:2308.06721*, 2023. 2, 4
- [47] Ge Yuan, Xiaodong Cun, Yong Zhang, Maomao Li, Chenyang Qi, Xintao Wang, Ying Shan, and Huicheng Zheng. Inserting anybody in diffusion models via celeb basis. *arXiv preprint arXiv:2306.00926*, 2023. 2
- [48] Kaipeng Zhang, Zhanpeng Zhang, Zhifeng Li, and Yu Qiao. Joint face detection and alignment using multitask cascaded convolutional networks. *IEEE signal processing letters*, 23(10):1499–1503, 2016. 12
- [49] Lvmin Zhang, Anyi Rao, and Maneesh Agrawala. Adding conditional control to text-to-image diffusion models. In *Proceedings of the IEEE/CVF International Conference on Computer Vision*, pages 3836–3847, 2023. 2, 3

- [50] Yufan Zhou, Ruiyi Zhang, Tong Sun, and Jinhui Xu. Enhancing detail preservation for customized text-to-image generation: A regularization-free approach. *arXiv preprint arXiv:2305.13579*, 2023. [2](#)

Appendix

A. Additional Experiment Setups

A.1. Training Dataset

Our training set comprises a robust collection of images, totaling 17 million single-person and 1.95 million multi-person instances. These images are sourced from both purchased data and publicly available sources. Each image has been carefully cropped and resized according to predefined specifications and subsequently organized into distinct data buckets based on shape categories. BLIP-2 [21] is employed to obtain image captions.

Face localization in images is performed using the MTCNN framework [48]. For generating the pose conditions, we employ the HRNet-DEKR model [11] for pose estimation. To enhance the accuracy of this estimation, we compute the average distance between facial keypoints detected by MTCNN (considered as ground truth) and those estimated by HRNet-DEKR. Poses with a large keypoint distance are filtered out to ensure precision.

A.2. Implementation Details

The network is trained using 8 NVIDIA H100 GPUs with batch size=4, learning rate=1e-05, weight decay = 0.01, using AdaFactor optimizer [36]. We train it for 720k iterations for stage 1, and stage 2 usually converges around 1 million iterations. We select the best model based on a 20 people validation set.

Because there is no official publicly available code for InstantFamily [17], for fairness, we implemented it based on the SDXL base model [29], and trained it using the same training data as our model.

B. Additional Quantitive Results

Details regarding the text alignment scores with varying numbers of faces are illustrated in Fig. A1. It is evident that all three methods exhibit comparable performance in terms of text alignment. Beside, we do not observe a significant change of the text alignment score across different number of faces.

C. Additional Visualizations

Additional pose-free generated images of our proposed ID-Patch can be found in Fig. A2, where the generation is conditioned on individual face locations while corresponding head sizes and body poses are inferred implicitly. Our method can accommodate a large number of people with diverse ethnic backgrounds, yet generating visually appealing group photo results.

Additional comparisons of pose-conditioned generated images are available in Fig. A3 and Fig. A4. In these vi-

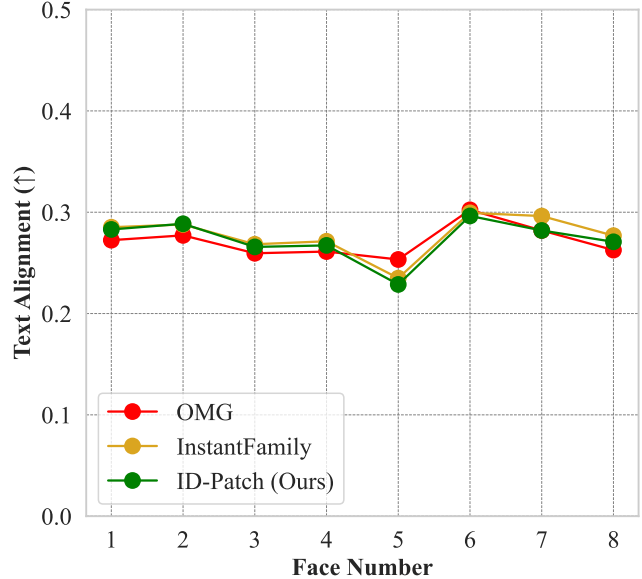


Figure A1. Performance evaluation of different model generations from the perspective of the text alignment score. There is no significant trend or difference between different number of faces. All methods achieve similar scores.

ualizations, our proposed method, ID-Patch, consistently achieves robust ID association without ID leakage. In contrast, the other two methods experience significant ID leakage as the total number of faces in the generated images increases.

| | | |
|---------------------------------|-----------------------------------------------------------------------------------------------------------------------------------------------------------------|------------------------------------------------------------------------------------------------------------------------------------------------------------------|
| <p>ID + ID Location</p> |  <p><i>“a male doctor, with a stethoscope”</i></p> |  <p><i>“four friends in chic outfits enjoying a night out”</i></p> |
| <p>Generation Result</p> |  |  |
| <p>ID + ID Location</p> |  <p><i>“group photo of six women in a sophisticated bar setting”</i></p> |  <p><i>“seven stylish young adults in an upscale indoor setting”</i></p> |
| <p>Generation Result</p> |  |  |

Figure A2. Additional visualizations of ID-Patch pose-free generation. Here the condition image is only ID patches rendered onto a black canvas without any pose condition.

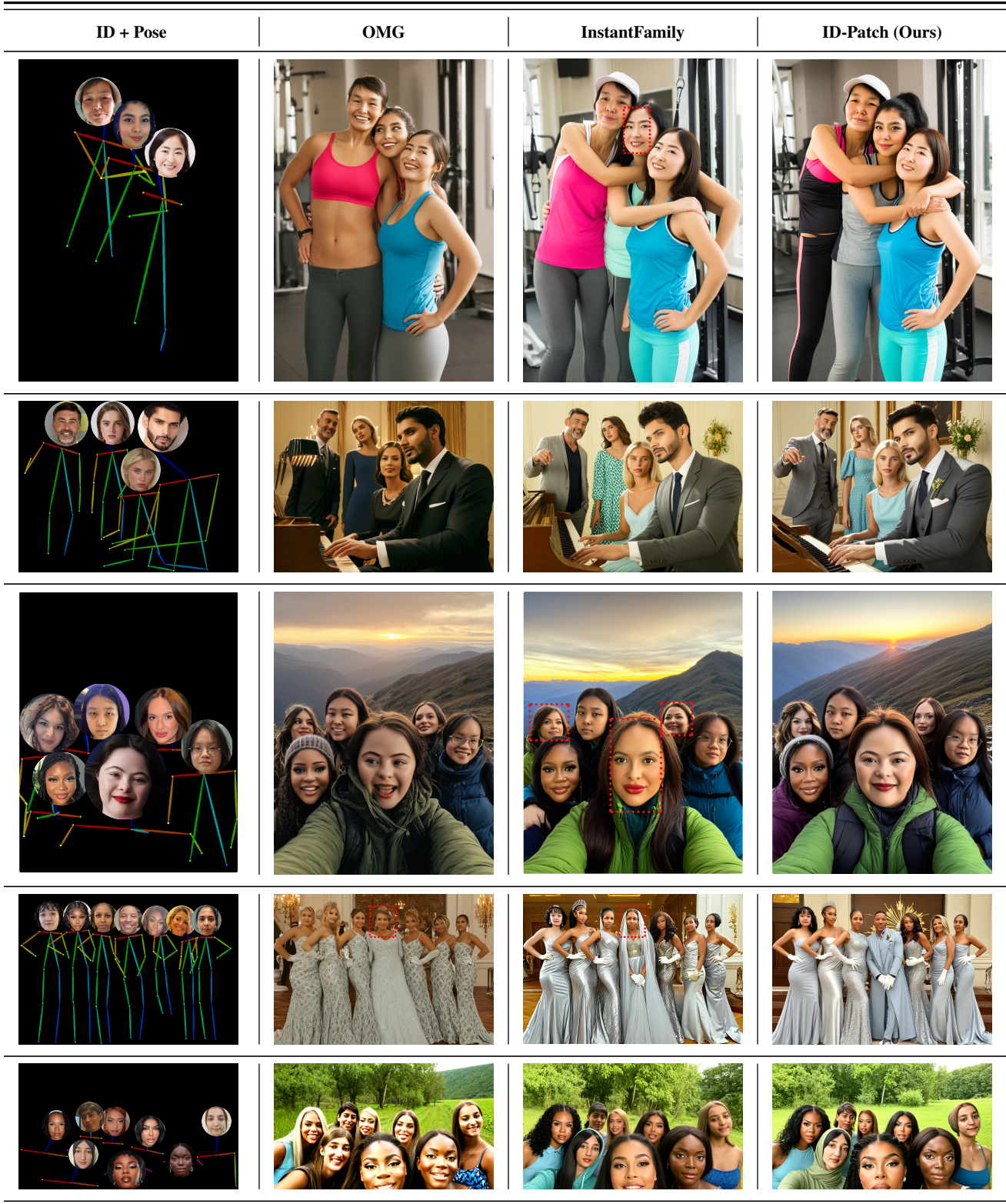


Figure A3. Part I: Additional comparison with baselines on pose-conditioned generation, where red dashed boxes highlight instances with low identity resemblance.

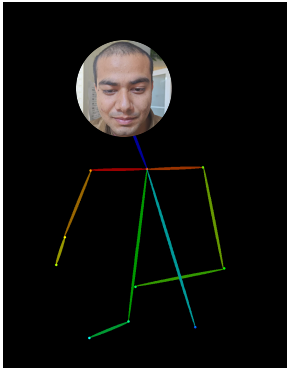
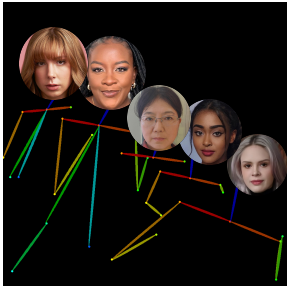
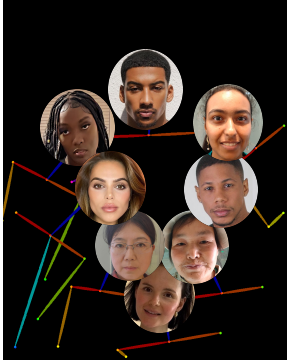
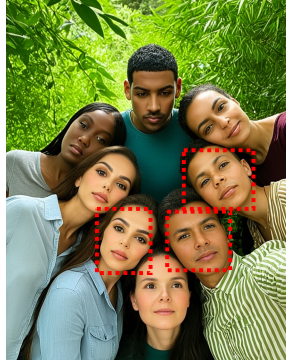
| ID + Pose | OMG | InstantFamily | ID-Patch (Ours) |
|-------------------------------------------------------------------------------------|-------------------------------------------------------------------------------------|--------------------------------------------------------------------------------------|---------------------------------------------------------------------------------------|
|  |  |  |  |
|  |  |  |  |
|  |  |  |  |
|  |  |  |  |

Figure A4. Part II: Additional comparison with baselines on pose-conditioned generation, where red dashed boxes highlight instances with low identity resemblance.